Observation of K x rays from highly ionized states of neon produced by 40-MeV Cl^{+7}, Cl^{+11}, and Cl^{+13} beams*

M. D. Brown, J. R. Macdonald, and Patrick Richard
Department of Physics and Nuclear Science Laboratory, Kansas State University, Manhattan, Kansas 66506

J. R. Mowat and I. A. Sellin
Department of Physics, University of Tennessee, Knoxville, Tennessee 31916,
Oak Ridge National Laboratory, Oak Ridge, Tennessee 37830
(Received 5 July 1973)

The K x-ray transitions of neon produced in single collisions of 40-MeV Cl^{+7}, Cl^{+11}, and Cl^{+13} beams with neon targets are resolved into eight components. Over half the x-ray production is found to be associated with the two- and three-electron system in all cases. Strongly charge-dependent neon Ly-α production is also observed. X-ray and vacancy-production cross sections are obtained for each component separately. We show that the vacancy-production cross section rather than the change in fluorescence yield dominates the charge dependence of the x-ray yields.

I. INTRODUCTION

A strong unexpected dependence of collisional x-ray yields upon the electronic configuration of the incident projectile has recently been discussed.[1-4] It was first reported[1] for 35.7-MeV fluorine ions in charge states ranging from F^{+5} to F^{+9} in thin gas targets of argon, krypton, and xenon, and independently[2] at about the same time for Ar^{+6} vs $\approx Ar^{+14}$ ions in neon. For 12–68-MeV oxygen projectiles incident on solid aluminum targets, a similar phenomenon has been observed.[3] The largest change in target x-ray yield was observed[4] when ≈80-MeV argon ions in charge states from +6 to +17 bombarded neon. The 60-fold increase in the observed neon K x-ray yield was explainable in part as an increase in the ionization state and hence the effective fluorescence yield of the neon states. The fluorescence-yield change was a barely satisfactory explanation, since only maximal fluorescence-yield changes could come close to explaining the large x-ray-yield increases. A recent high-resolution measurement of 30-MeV oxygen on Ne demonstrated that the Ne vacancy production depends very strongly on the oxygen projectile charge state.[5] The relative population of states with one K shell and various numbers of L-shell vacancies changes when the electronic configuration of the projectile changes. None of the low-resolution experiments can distinguish fluorescence-yield effects from basic vacancy-production increases. The need to resolve this ambiguity provided the stimulus for the work reported here, which demonstrates the inadequacy of fluorescence-yield arguments taken alone.

We report high-resolution measurements of neon K x-rays produced by fast chlorine-ion beams. Eight lines of the neon K x-ray spectrum are observed when 40 MeV, Cl^{+7}, Cl^{+11}, and Cl^{+13} ions bombarded neon. Over half the x-ray intensity is associated with two- and three-electron neon ions in all cases. No x rays are observed from neon systems with more than five electrons. With increasing projectile charge state, the neon system is left in successively higher states of ionization, and no transitions from the five-electron neon system are observed in the spectra when Cl^{+13} ions are incident. The production of such highly ionized systems is also evidenced by a rapid growth with increasing projectile-charge state of the hydrogenic neon Ly-α line produced most abundantly by the Cl^{+13} beam. X-ray and vacancy-production cross sections have been derived for each observed line.

II. EXPERIMENTAL PROCEDURE

In this experiment, 40-MeV chlorine ions from the Kansas State University Tandem Van de Graaff accelerator were selected by the switching magnet in a specific charge state (i.e., Cl^{+7}, Cl^{+11}, or Cl^{+13}) and directed through a differentially pumped gas cell to a Faraday cup. The interaction region was viewed by a curved-crystal spectrometer[6] fitted with a rubidium acid phthalate (RAP) crystal to disperse the x rays and a flow-mode proportional counter with a 2.0-μm Siemens foil window to detect the x rays. To maximize the x-ray yield while still approximating single collision conditions, the pressure in the gas cell was maintained at ≈100 μ. A Si(Li) detector, which also viewed the interaction region, detected both neon and

chlorine K x rays. Since the total number of x rays viewed by this detector is proportional to the product of beam intensity and target density, the counts registered in this detector were used for normalization of all spectra. Fluctuations in beam-current and gas-cell pressure are eliminated from the data by normalizing to total x rays in this manner. Multichannel spectra were accumulated from the crystal spectrometer with the number of x rays counted at a particular setting corresponding to a fixed number of chlorine and neon x rays detected in the Si(Li) detector. The energy resolution in the region of interest is about 10-eV full width at half-maximum (FWHM). In this experiment the observed intensity for each component was corrected for a crystal reflectivity[7] that ranged from 8.1×10^{-5} to 10×10^{-5} and for absorption in the 2.0 μm window of the proportional counter that ranged from 62% at 881 eV to 46% at 1079 eV.

III. RESULTS

In Fig. 1 are shown the neon K x-ray spectra produced by 40-MeV Cl^{+7}, Cl^{+11}, and Cl^{+13} on neon in the gas cell. The spectra contain two groups of lines. In the energy region from 870 to 930 eV, four of the neon satellite transitions have been[5] identified as KL^4, KL^5, KL^6, and KL^7, where the notation KL^n corresponds to the defect configuration of one K-shell vacancy and n L-shell vacancies. This satellite notation, which is used here for convenience, is questionable. Cocke *et al.*[8] have found, in their study of the lifetime of the $(1s^2\,2s)\,^2S$-$(1s2s2p)\,^4P$ transition in sulfur, that the splitting between quartet and doublet states is comparable to the average splitting for two defect configurations. Examination of the spectroscopy of few electron systems reveals a large energy range for a given defect configuration.

An overlap of the transitions for different defect configurations occurs in neon. The KL^7 satellite centered at 919 eV is a combination of the $(1s^2)\,^1S$-$(1s2p)\,^1P$ transition at 922 eV[9] and the $(1s^2)\,^1S$-$(1s2p)\,^3P$ transition at 915 eV,[9] both in heliumlike neon. Metastable states such as the $(1s2p)\,^3P$ in heliumlike neon are detected in this experiment if the radiation occurs before the recoiling neon ion leaves the field of view of the detector. The $(1s2s)\,^3S$ state has a long lifetime and decays primarily by $2E1$ decay to the ground state with a total energy of 905 eV[10] and would not be detected in the KL^6 satellite centered at 909 eV in the present experiment. The $(1s^2 2p)\,^2P$-$(1s2p^2)\,^2P$ transition at 908 eV[11] and the $(1s^2\,2s)\,^2S$-$(1s2s2p)\,^4P$ transition at 897 eV[11] both in lithiumlike neon should contribute to KL^6 and KL^5, respectively.

The four-electron neon transition $(1s^2\,2s^2)\,^1S$-$(1s2s^2\,2p)\,^1P$ at 896 eV[12] also contributes to KL^5 centered at 897 eV. Clearly splitting between different multiplets is comparable to the separation of the average energy between two adjacent defect configurations. This means that a particular KL^n line may arise from ions of different charge states. In particular KL^5 may be composed of transitions from three- and four-electron neon. Table I contains a summary of these considerations. Further experimental measurements are necessary to unfold the details of these spectral features.

In the energy region from 1000 to 1090 eV, a second group of four transitions corresponding to transitions between one-, two-, three-, and four-electron neon states is observed to increase from 13% of the total intensity for Cl^{+7} to 22% for Cl^{+13}. The hydrogenlike neon Lyman-α transition at 1022 eV (unresolved in the Cl^{+7} spectrum) grows in intensity more than any other spectral feature as the charge state is increased. It is

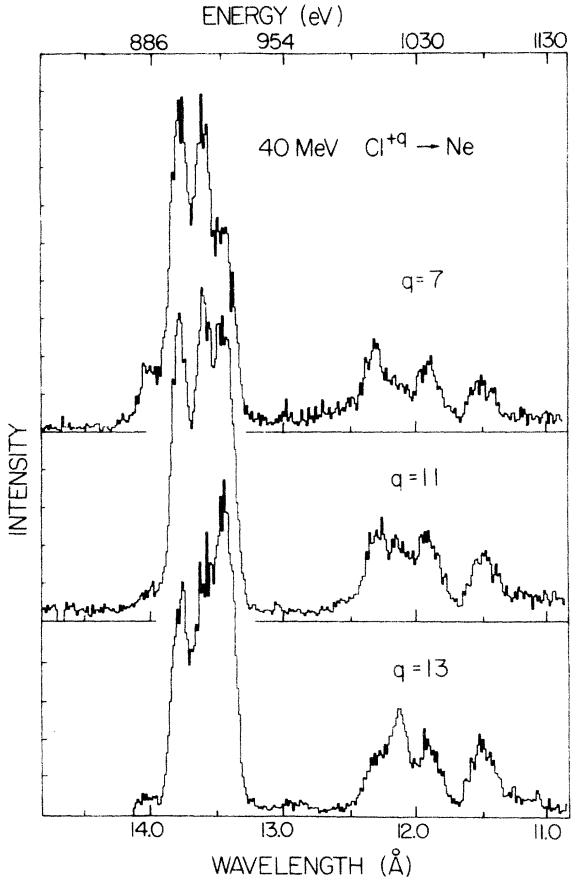

FIG. 1. Neon K x-ray spectra resulting from collisions of 40-MeV Cl^{+7}, Cl^{+11}, and Cl^{+13} beams with a neon gas target. The spectra displayed in equal wavelength intervals cover the energy range from about 820 to 1150 eV.

TABLE I. Identification, calculated energies of some of the multiplet states for the two-electron, three-electron and four-electron configurations, and observed energies are presented.

		Calculated transition energies					
Peak assignments	Ionic state	Final state		Initial state	Energy (ev)	Ref.	Observed energy (eV)
KL^7	He-like	$(1s^2)\,^1S$	-	$(1s2p)\,^1P$	922	9	919
	He-like	$(1s^2)\,^1S$	-	$(1s2p)\,^3P$	915	9	
KL^6	Li-like	$(1s^2 2p)\,^2P$	-	$(1s2p^2)\,^2P$	908	11	909
	He-like	$(1s^2)\,^1S$	-	$(1s2s)\,^3S$	905	10	
KL^5	Li-like	$(1s^2 2s)\,^2S$	-	$(1s2s2p)\,^4P$	897	11	897
	Be-like	$(1s^2 2s^2)\,^1S$	-	$(1s2s^2 2p)\,^1P$	896	12	

the most intense line in this energy region when excited with the 40-MeV Cl^{+13} beam. The highest energy peak observed at 1079 eV is identified as the $(1s^2)\,^1S_0$-$(1s3p)\,^1P_1$ transition in the heliumlike neon system. The other two lines observed at 1009 and 1040 eV are consistent with the $(1s^2 2s^2)\,^1S_0$-$(1s2s^2 3p)\,^1P_1$ transition in the four-electron system and the $(1s^2 2s)\,^2S_{1/2}$-$(1s2s3p)\,^2P$ transition in the three-electron system, respectively.

In Table II the observed energy, identification, relative intensity, and average calculated fluorescence yield for each resolved line are summarized. The fluorescence yield listed cannot be entirely correct, since the multiplicity splitting causes a mixing of the defect configurations among the lines. Even if a particular line could be identified, no fluorescence-yield calculations exist for a particular transition in these neon systems. Fortunately, the calculated[13] fluorescence yields for most of the defect configurations do not vary much. The fluorescence yields for KL^4, KL^5, and KL^6 listed in Table II are average fluorescence yields (ω_n) obtained by statistically weighting the calculated[13] fluorescence yields for still unresolved components of each defect configuration, as given by Kauffman *et al.*[5] The fluorescence yield for KL^7 and Lyman-α are unity. The relative intensities listed in Table II are normalized to the total x-ray intensity observed.

From the relative intensities given in Table II, a semiempirical effective fluorescence yield $\bar{\omega}$ can be derived[5] using the equation

$$\frac{1}{\bar{\omega}} = \sum_n \frac{R_n}{\omega_n},$$

where R_n are the relative intensities and ω_n are the statistically weighted fluorescence yields listed in Table II. The distribution of configurations which produce each line has been chosen the same for the different projectile charge states. In this manner, we find $\bar{\omega} \approx 4\omega_0$ for Cl^{+7}, $\bar{\omega} \approx 5\omega_0$ for Cl^{+11}, and $\bar{\omega} \approx 6\omega_0$ for Cl^{+13}, where $\omega_0 = 0.018$ is the experimental value[14] of the neon atomic fluorescence yield. These three effective flu-

TABLE II. Observed energy, identification, average flourescence yield (ω_n), intensity of each line relative to the total line intensity, the x-ray-production cross section, and the vacancy-production cross section listed for each neon K x-ray line when neon was bombarded by 40-MeV Cl^{+7}, Cl^{+11}, and Cl^{+13} beams. The x-ray-production cross sections are normalized (Ref. 16 and 17) to total x-ray-production cross sections obtained with Si(Li) detectors.

			Relative intensity			x-ray production cross section (10^{-19} cm^2)			vacancy production cross section (10^{-18} cm^2)		
Observed energy (eV)	Identification	ω_n	Cl^{+7}	Cl^{+11}	Cl^{+13}	Cl^{+7}	Cl^{+11}	Cl^{+13}	Cl^{+7}	Cl^{+11}	Cl^{+13}
881	KL^4	0.029	0.05	0.02	0.00	0.11	0.1	0.0	0.4	0.4	0.0
897	KL^5	0.042	0.32	0.26	0.22	0.73	1.8	3.2	1.7	4.3	7.6
909	KL^6	0.083	0.30	0.27	0.26	0.66	1.9	3.7	0.8	2.2	4.4
919	KL^7	1.000	0.20	0.26	0.30	0.44	1.8	4.3	0.04	0.1	0.4
1009	a	1.000	0.05	0.06	0.04	0.11	0.4	0.6	0.01	0.04	0.06
1022	$1s\,^2S_{1/2}$-$2p\,^2P_{3/2}$	1.000	0.02	0.05	0.08	0.05	0.3	1.1	0.005	0.03	0.1
1040	a	1.000	0.04	0.05	0.05	0.08	0.4	0.6	0.008	0.04	0.06
1079	$1s^2\,^1S_0$-$1s3p\,^1P_1$	1.000	0.02	0.04	0.05	0.05	0.3	0.8	0.005	0.03	0.08
					Total	2.2	6.9	14.	3.	7.	13.

[a] The identification for this transition is not definite; the fluorescence yield has been assumed to be unity.

orescence yields are the largest observed for heavy ion collisions with neon. They may be compared with the values[5] $\bar{\omega} = 2.5\omega_0$, $2.8\omega_0$, and $3.2\omega_0$ for 30-MeV O^{+5}, O^{+7}, and O^{+8} beams or the value[15] $\bar{\omega} = 2.4\omega_0$ obtained from Auger-electron and x-ray spectra of 30-MeV oxygen on neon. For all but doubly excited two-electron neon ions, and all one-electron neon ions, $\omega = 56\omega_0 = 1$. The 50% increase in the fluorescence yield observed with increasing projectile-charge state is caused not so much by increased production of highly ionized states of neon, but rather the absence of low states of ionization. The fluorescence yield increases with charge state because the intensity of the KL^4 satellite decreases and the KL^5 satellite becomes relatively weaker.

To proceed to x-ray-production and vacancy-production cross sections, total x-ray-production cross sections at each charge state are required for normalization. We have accomplished this by using the total neon K x-ray-production cross sections measured with Si(Li) detectors at 40-MeV[16] for Cl^{+7} and at 42-MeV[17] for Cl^{+11} and Cl^{+13}. The cross sections at 42 MeV differ little from those at 40 MeV, since the cross sections are nearly the same[17] for both Cl^{+11} and Cl^{+13} beams at 42 and 50 MeV. The spectral shape in the unresolved Si(Li) detector data could be deduced from the relative intensities determined in this high-resolution experiment permitting improvement of necessary window-transmission corrections. The window-transmission factor was recalculated for the Si(Li) detectors, and the corrected x-ray production cross sections obtained in this manner were 2.2×10^{-19}, 6.9×10^{-19}, and $14 \times 10^{-19}\,\mathrm{cm}^2$ for Cl^{+7}, Cl^{+11}, and Cl^{+13}, respectively. These total cross sections which increase six-fold as the chlorine charge state goes from 7 to 13 were used for normalization to derive the x-ray-production cross section for each component listed in Table I. A skewing of the satellite distribution to higher states of ionization occurs as the cross section for the KL^4 satellite decreases, while that for the KL^5, KL^6, and KL^7 components increase by factors of 4, 5, 10, respectively, as the projectile charge is raised. The cross section for the Lyman-α transition increases by a factor of 20, while those for the other high-energy lines increase by somewhat smaller amounts as the projectile charge increases. The observation of hydrogenic Lyman-α radiation indicates that these collisions are violent. The hydrogenic neon may be produced by removing nine electrons and exciting the remaining electron, or by removing all ten electrons with a subsequent electron capture by the bare neon nucleus. In either case, this strong charge-state dependence is consistent with an increase in the interaction strength when the incident projectile charge state is increased.

K-shell vacancy-production cross sections listed in Table II were calculated for each component using the average fluorescence yields from the table. The total vacancy-production cross section was found to increase from $3 \times 10^{-19}\,\mathrm{cm}^2$ for Cl^{+7} to $7 \times 10^{-18}\,\mathrm{cm}^2$ for Cl^{+13}. For comparison, the inner-shell ionization cross section calculated in the plane-wave Born approximation[18] for fully stripped 40-MeV chlorine on neon is $24 \times 10^{-18}\,\mathrm{cm}^2$. The large change in the vacancy-production cross section and the final target configuration with the electronic structure of the projectile, indicates that many electrons are active in these collisions. The fact, that no x rays are observed from neon states with more than five electrons, dictates that the chlorine projectile must remove many L-shell electrons when it removes a single K-shell electron.

IV. SUMMARY

In summary, we have resolved into eight components the K x-ray transitions of neon produced in single collisions of 40-MeV Cl^{+7}, Cl^{+11}, and Cl^{+13} beams with neon targets. The neon is always observed in high states of ionization. The two- and three-electron systems account for over half the observed x-ray intensity in all cases. A strongly charge-state dependent neon Lyman-α production is also observed. For each separate component, vacancy- and x-ray-production cross sections are determined. We have combined high-resolution x-ray spectra with data taken with a Si(Li) detector to separate the contributions of changes in fluorescence yield and vacancy production to the charge-state dependence of the x-ray yields observed in ion-atom collisions. Since the effective fluorescence yield increases only 50% for the incident chlorine states used in this experiment, we conclude that the strong charge dependence of observed x-ray production[4] is dominated by the increase in vacancy-production cross section.

ACKNOWLEDGMENTS

The authors are grateful to Dr. C. L. Cocke and Dr. B. Curnutte for sharing their unpublished results and for many stimulating discussions. We are happy to acknowledge discussions with Dr. C. P. Bhalla on his fluorescence-yield results.

*Work partially supported by the U. S. Atomic Energy Commission under Contract No. AT(11-1)-2130, and by the Office of Naval Research.

[1]J. R. Macdonald, L. Winters, M. D. Brown, T. Chiao, and L. D. Ellsworth, Phys. Rev. Lett. 29, 1291 (1972).

[2]J. R. Mowat, D. J. Pegg, R. S. Peterson, P. M. Griffin, and I. A. Sellin, Phys. Rev. Lett. 29, 1577 (1972).

[3]W. Brandt, R. Laubert, M. Maurino, and A. Schwarzschild, Phys. Rev. Lett. 30, 358 (1972).

[4]J. R. Mowat, I. A. Sellin, D. J. Pegg, R. S. Peterson, M. D. Brown, and J. R. Macdonald, Phys. Rev. Lett. 30, 1289 (1973).

[5]R. L. Kauffman, F. Hopkins, C. W. Woods, and P. Richard, Phys. Rev. Lett. 31, 621 (1973).

[6]J. L. Jones, K. W. Paschen, and J. B. Nicholson, Appl. Opt. 2, 955 (1963).

[7]Based on measurements by R. L. Blake (unpublished).

[8]C. L. Cocke, B. Curnutte, R. Randall, and J. Bednar (unpublished).

[9]R. C. Elton, Astrophys. J. 148, 573 (1967).

[10]Y. Accad, C. L. Perkeris, and B. Schiff, Phys. Rev. A 4, 516 (1971).

[11]A. H. Gabriel and Carole Jordan, Nature (Lond.) 221, 947 (1969).

[12]Lewis L. House, Astrophys. J. Suppl. 18, 21 (1969).

[13]C. P. Bhalla and M. Hein, Phys. Rev. Lett. 30, 39 (1973); C. P. Bhalla, N. O. Folland, and M. A. Hein, Phys. Rev. A 8, 649 (1973).

[14]J. Heinz, Z. Phys. 143, 153 (1955).

[15]D. Burch, W. B. Ingalls, J. S. Risley, and R. Heffner, Phys. Rev. Lett. 29, 1719 (1972).

[16]L. Winters, J. R. Macdonald, M. D. Brown, T. Chiao, L. D. Ellsworth, and E. W. Pettus, Phys. Rev. Lett. 31, 1344 (1973).

[17]J. R. Mowat, I. A. Sellin, P. M. Griffin, D. J. Pegg, and R. S. Peterson (unpublished).

[18]E. Merzbacher and H. W. Lewis, in *Handbuch der Physik*, edited by S. Flügge (Springer, Berlin, 1958), Vol. 34, p. 166.